# Contraction Stress Build-Up of Anisotropic Conductive Films (ACFs) for Flip-Chip Interconnection: Effect of Thermal and Mechanical Properties of ACFs

**Woon-Seong Kwon, Kyung-Wook Paik**

*Department of Materials Science and Engineering, Korea Advanced Institute of Science and Technology, 373-1, Guseong-dong, Yuseong-gu, Daejon 305-701, Korea*

Received 00 Month 0000; accepted 00 Month 2004
DOI 10.1002/app.20844
Published online in Wiley InterScience (www.interscience.wiley.com).

**ABSTRACT:** The important mechanical mechanism for the electrical conduction of anisotropic conductive films (ACFs) is the joint clamping force after the curing and cooling processes of ACFs. In this study, the mechanism of shrinkage and contraction stress and the relationship between these mechanisms and the thermomechanical properties of ACFs were investigated in detail. Both thickness shrinkages and modulus changes of four kinds of ACFs with different thermomechanical properties were experimentally investigated with thermomechanical and dynamic mechanical analysis. Based on the incremental approach to linear elasticity, contraction stresses of ACFs developed along the thickness direction were estimated. Contraction stresses in ACFs were found to be significantly developed by the cooling process from the glass-transition temperature to room temperature. Moreover, electrical characteristics of ACF contact during the cooling process indicate that the electrical conduction of ACF joint is robustly maintained by substantial contraction stress below $T_g$. The increasing rate of contraction stresses below $T_g$ was strongly dependent on both thermal expansion coefficient (CTE) and elastic modulus ($E$) of ACFs. A linear relationship between the experimental increasing rate and $E \times$ CTE reveals that the build-up behavior of contraction stress is closely correlated with the ACF material properties: thermal expansion coefficient, glassy modulus, and $T_g$. © 2004 Wiley Periodicals, Inc. J Appl Polym Sci 93: 2634–2641, 2004

**Key words:** anisotropic conductive films (ACFs); stress; shrinkage; thermomechanical properties; glass transition

## INTRODUCTION

Anisotropic conductive films (ACFs) have been extensively used in LCD display packaging areas, contactless smart-card module assemblies, and bare chip attachments on flexible and rigid substrates. They consist of an adhesive polymer matrix and fine conductive fillers of metallic, or metal-coated polymer, particles, and when used for integrated circuit assembly provide electrical conduction as well as mechanical interconnections.[1] As schematically shown in Figure 1, electrical conduction is provided by the deformation of the conductive particles trapped between the chip bumps and substrate pads in the $z$-axis of the adhesives perpendicular to the plane of the board, whereas electrical isolation is maintained in the plane of the adhesive layer.[2–4] In addition, electrical interconnections are mechanically constructed by the solidification of the adhesive polymer matrix caused by curing and cooling, which builds up sufficient contractive force to establish stable and low-resistance electrical connections. In other words, anisotropic conductive films contract and solidify during the curing and cooling processes, so that adhesive shrinkage in the cured ACFs leads to electrical joint clamping. Herein, contractive force developed in the ACF during the assembly process causes the conductive particles to be in a compressed state but the adhesive matrix in a stretched state. The contractive forces, shown by A and B in Figure 1, must be high enough to maintain the mechanical contact by balancing the epoxy contraction (A and B) and the particles' elasticity characteristics (a–h). Therefore, the bonding quality of electrical contacts through the deformation of conductive particles depends on the contractive force established by thermal shrinkage of the ACFs after curing and cooling.

However, a fundamental understanding about this contractive force, developed along the $z$-axis after curing and cooling of ACF, is still lacking. The critical sources of the contractive force (joint clamping force) that establish the ACF electrical conduction originate from thermomechanical properties such as thermal shrinkage and build-up stiffness during or after thermal reaction of ACFs. In other words, the magnitude and behavior of the contractive force developed in ACFs are dependent on a number of factors. These factors include thermal and mechanical properties,

*Correspondence to:* W.-S. Kwon (wskwon@kaist.ac.kr).

Journal of Applied Polymer Science, Vol. 93, 2634–2641 (2004)

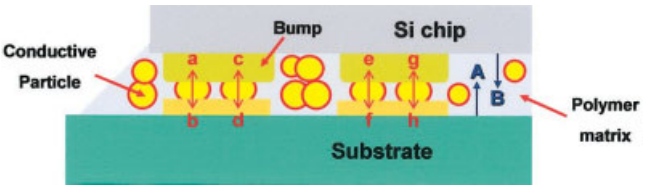


**Figure 1** Schematic of conduction mechanism of flip-chip joint with anisotropic conductive films (ACFs). A and B: Contractive forces of ACFs; a–h: repulsive forces of compressed conductive particles.

such as glass-transition temperature, thermal expansion coefficients, and elastic modulus of ACFs. To understand and design a reliable ACF joint, the development of *z*-axis contraction stress should be quantitatively understood, with the consideration of shrinkage behavior and thermomechanical properties.

In this study, the mechanism of shrinkage and contraction stress, and the relationship between these behaviors and the thermomechanical properties of ACFs, are investigated in detail.

## RESEARCH BACKGROUND

One way to estimate the magnitude and behavior of internal stress in ACFs for electronic packaging applications is to use equations of linear elasticity. During the curing and cooling processes of epoxy-based ACFs, however, thermal and mechanical properties change dramatically. As the curing reaction proceeds, cure shrinkage and significant modulus increase occur, as a result of the decrease of free volume and the formation of crosslinked molecular structure, respectively. ACFs, upon cooling from curing temperature to room temperature, change from a rubbery state to a glassy state. The glass transition is accompanied by both physical shrinkage and an increase in glassy modulus. These dramatic changes in thermal and mechanical properties obstruct the use of the general stress–strain equations of linear elasticity. An appropriate way to elude this problem is to use an incremental approach to linear elasticity.[1] In this incremental approach, the stress increment is calculated from strain increments over an infinitesimal interval in which the material properties are assumed to be constant. The subsequent stress state is the accumulation of all the incremental stress values.

The evolution of contractive force in epoxy-based ACFs typically involve two steps with respect to thermal and mechanical properties: (1) curing at an elevated bonding temperature where ACFs chemically shrink and build up stiffness; (2) cooling from elevated bonding temperature to room temperature where ACFs physically shrink and become stiff.

The cured ACFs in the rubbery state, just after completion of the curing reaction, have a low rubbery modulus, and consequently the contractive force that developed during the curing reaction is almost negligible. In the cooling process from $T_g$ to room temperature, the contractive force may be considerably developed as a result of the thermal shrinkage and significant increase in glassy modulus.

The contraction stress of epoxy resin that originated from the curing and cooling processes is also affected by how the epoxy resin is constrained in the specific structure.[5] Actually, the ACF layer is structurally constrained between the chip and substrate, which are generally more rigid than ACF polymeric materials. It is therefore worth noting that the thickness shrinkage along the *z*-axis of the ACF layer in such a flip-chip structure is a characteristic not only of the ACF layer but also of the system, that is, the ACF layer, chip, and substrate together. Thermal contraction of the ACF layer along the *z*-axis at such a constrained structure is different from that of ACF in the free-standing state. It means that the contraction stress of ACF materials along the thickness direction under constrained structure may be different from the stress derived from the simple Hook's law, under the following assumptions: materials isotropy, incrementally linear elastic behavior, history-dependent elastic coefficients, and no viscoelastic behavior. The magnitude of contraction stresses also depends on the thermal and mechanical properties such as coefficient of thermal expansion (CTE), elastic modulus ($E$), and glass-transition temperature ($T_g$).[6,7]

Accordingly, in estimating the contraction stress of ACF materials along the *z*-axis in a constrained structure, both the constraint effect and viscoelastic property of ACF materials should be considered. In this study, by measuring the thickness shrinkage along the *z*-axis under constrained structure, contraction stress of the ACF layer along the thickness direction was calculated based on the incremental approach to linear elasticity.

In this contribution, we establish a methodology on which one could depend to predict the contraction stresses with the known materials properties by constructing the relationship between contraction stresses and thermomechanical properties.

## EXPERIMENTAL

### Materials

An epoxy adhesive mainly composed of solid bisphenol-A, liquid bisphenol-F, and phenoxy resins was formulated to study the four ACFs (ACF-A, ACF-B, ACF-C, and ACF-D) with different thermal and mechanical properties. Two kinds of curing agent, $\alpha$ (ACF-A, ACF-B, and ACF-C) and $\beta$ (ACF-D), were added to epoxy-based resin to alter the thermal and mechanical properties of the cured ACFs. Then, stoi-

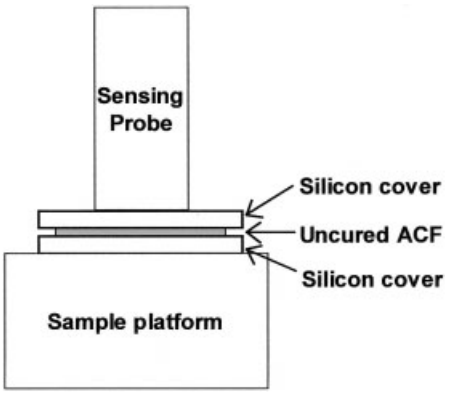


**Figure 2** Schematic of thermal shrinkage measurement setup of ACFs during curing and cooling processes.

chiometric amounts of the curing agent were mixed in the epoxy resin. The Au-plated polymer spheres (5 $\mu$m diameter) were also mixed with the formulated epoxy resin to produce a conductive adhesive of 5 wt % filler content. Silica particles (0.8 $\mu$m diameter) were used as a reinforcement filler to change the modulus and CTE of cured ACFs (ACF-B and ACF-C). The mixtures were stirred until the curing agent and additives were completely dissolved in the epoxy resin. The resin mixtures prepared by formulating epoxy-based resin, curing agents, conductive fillers, and additives were coated to a dried-film format on the carrier PET film. The ACFs used were about 50 $\mu$m in thickness.

### Thickness contraction measurements

Dimensional changes of ACFs during heating and cooling were monitored by a thermomechanical analyzer with thermal analysis software, over a temperature range from 30 to 180°C, at a heating rate of 5°C/min in $N_2$ gas environment (Fig. 2). ACFs with a size of 5 × 5 × 0.05 mm were held between two pieces of silicon cover. The static force applied to a sensing probe for the monitoring of *z*-directional changes was set to minimum value to prevent the squeeze-out of ACF. The *z*-directional change of only two silicon covers was also measured and subtracted from the total *z*-directional dimension changes to isolate only the *z*-directional shrinkage of ACFs. Because the upper and lower surface of the ACF sample were held to parallel silicon cover plates, where the shrinkage in the *x–y* plane is constrained, the uniaxial strain condition can be assumed for the free axial shrinkage condition. The *z*-directional shrinkage of ACFs during the curing and cooling processes could be obtained from the dimensional change of TMA measurement. Many repetitions of thickness change measurement confirmed that measurement of thickness contraction by TMA was experimentally reproducible, with a variation of less than 10%.

### Thermal expansion and dynamic mechanical measurements

Thermal expansion measurements of cured ACF samples (dimensions 2.5 × 15.0 × 0.05 mm) were made on a TMA/SS 6100 thermomechanical analyzer (Seiko Instruments, Chiba, Japan) at a heating rate of 5°C/min. Specimens were subjected to a uniaxial tension mode from 30 to 180°C. The CTE values were calculated from the linear section of thermal expansion versus temperature in the TMA curves.

Very thin (50 $\mu$m) ACF film strips (2.5 mm wide and 15 mm long) were characterized in the tension mode to determine the viscoelastic properties. In this mode, cured ACFs with film type were fastened vertically between the grips, and a sinusoidal stress was applied to the specimen. An initial tension of 200 mN was applied to the film and then the tension force oscillated ±100 mN at a frequency of 0.02 Hz. As the ACF specimen was heated at a heating rate of 5°C/min, the change in sample length was recorded with the cycling force. The data were then processed to determine the viscoelastic properties using the DMA software.

### ACF flip-chip assembly process

The dimensions of the silicon chips with four-point Kelvin structure were 10.0 × 10.0 × 0.7 mm. Electroplated gold bumps were formed on pads of a chip. The bump size was 150 $\mu$m in diameter and the bump pitch was 250 $\mu$m. After ACFs were placed onto a substrate, a chip and a substrate were aligned and bonded by applying heat (180°C) and pressure (2–3 N/bump) for 20 s. Figure 3 shows the cross-sectional view of the ACF assembly and a schematic view of contact resistance measurement. As shown in Figure 3, multiple conductive spheres were trapped between the gold bump and substrate pad. By using the circuit design for electrical measurement, contact resistance can be calculated as $V/I$. *In situ* contact resistance of ACF joint was measured with changing environmental temperature.

## RESULTS AND DISCUSSION

### Shrinkage behavior during curing and cooling processes

The *z*-directional thickness changes in the curing and cooling processes for four ACFs are illustrated in Figure 4. As shown in Figure 4, with increasing temperature, the ACF started to expand as a result of polymer chain movement. This early expansion of ACF has no significant contribution to the evolution of stress in ACFs. When ACFs acquired enough thermal energy for curing reaction to start, the ACFs started a crosslinking reaction to form a polymer network structure. When the curing reaction started

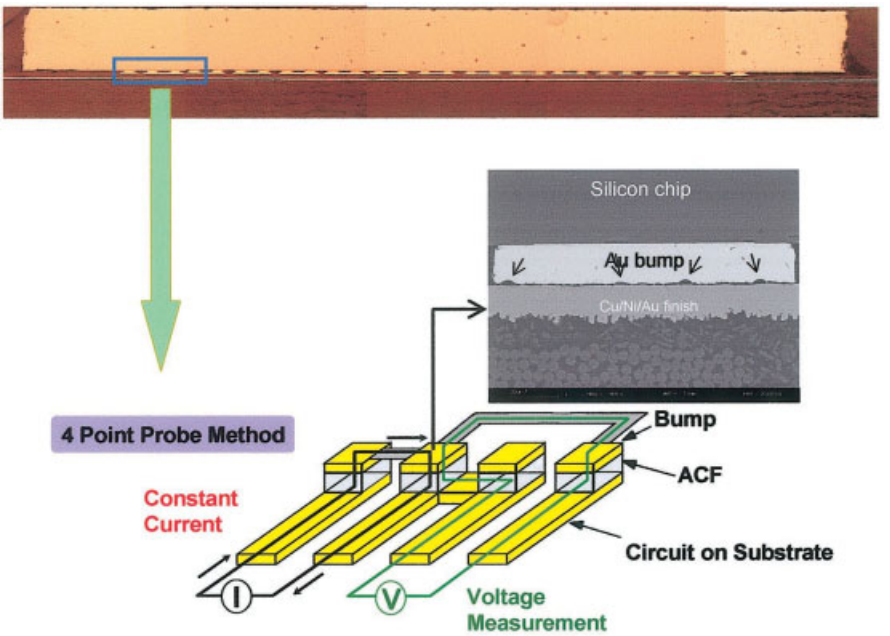


**Figure 3** Cross-sectional view of ACF assembly and four-point probing method for contact resistance measurement of single bump.

at about 100°C, cure shrinkage became detectable, as shown in Figure 4. Finally, as the cure reaction was completed, cure shrinkage attributed to the crosslinking reaction diminished. Cured ACFs then started to expand again in the rubbery region after completion of the curing reaction. During cooling to room temperature, thickness shrinkages exhibited two different slopes, differentiated by glass-transition temperature. It is worth noting that ACFs in the chip assembly process experience both cure shrinkage (chemical shrinkage), attributed to epoxy crosslinking, and thermal shrinkage (physical shrinkage), attributed to the cooling process, from the bonding temperature to room temperature. The shrinkage behaviors in the curing and cooling processes are depicted in detail in Figure 5(a) and (b), respectively. In all materials, the cure shrinkage ascribed to the crosslinking of epoxy chains transitionally increased at the beginning of curing. Then, ACFs rapidly shrunk with the progress of curing and attained constant degrees of shrinkage, ranging from 1.5 to 2.0%, when the curing reaction was completed. For all cured ACFs, the shrinkage versus temperature plots in the cooling process are represented by a straight line having one inflection point, as shown in Figure 5(b). The temperature where the inflection point was observed corresponds to the glass-transition temperature. The values of cure and cooling shrinkage are summarized in Table I. The four ACFs under investigation did not exhibit a significant difference in cure shrinkages because all ACF materials were based on a similar epoxy binder. As presented in Table I, the extent of cure shrinkages was almost smaller than that of cooling shrinkages. However, the substantial shrinkage after the curing and cooling processes does not directly imply high contraction stress because a polymer with high dilatometric variation generally leads to low elastic stiffness. Accordingly, the build-up behavior of contraction stress that developed during the cooling process should be investigated by taking into account not only the thermal shrinkage but also the temperature-dependent elastic modulus.

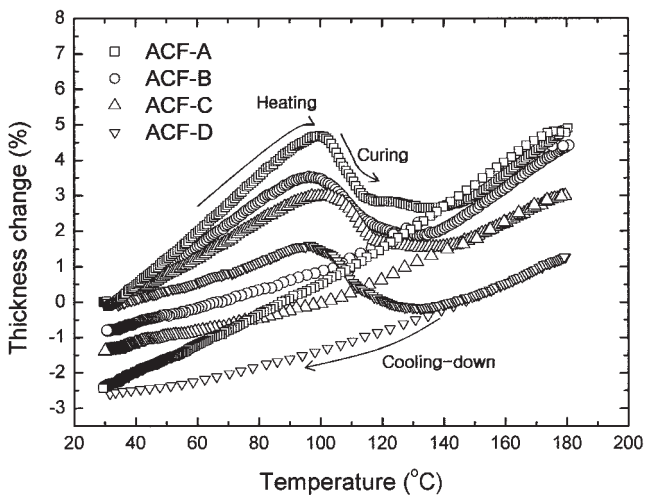


**Figure 4** Dimensional changes of four ACFs along the thickness direction during curing and cooling processes.

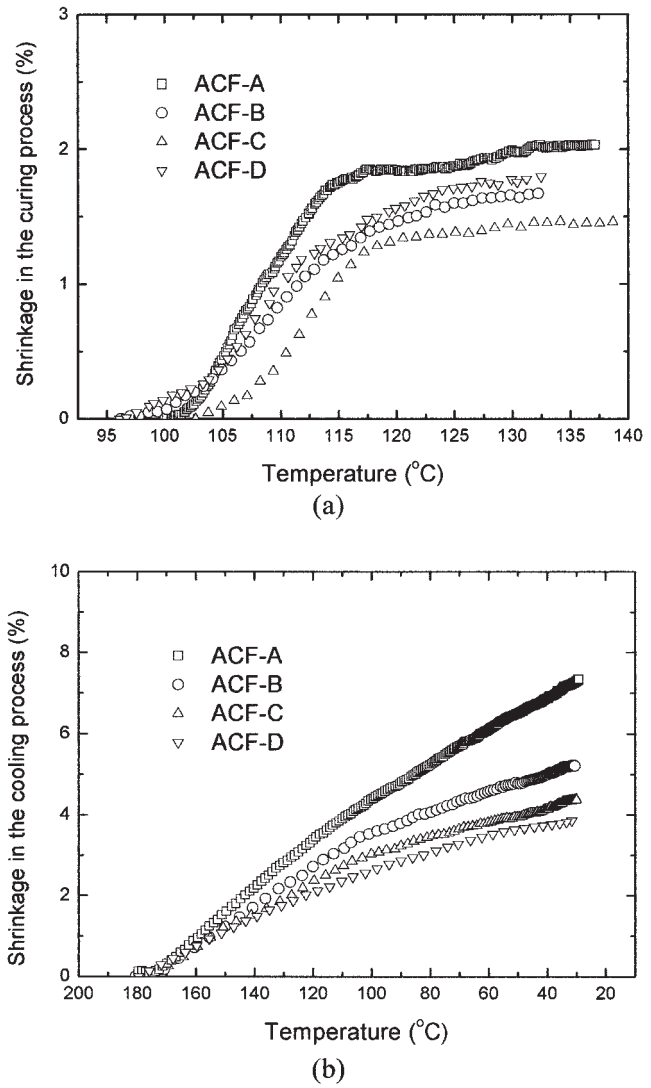


**Figure 5** Shrinkage behaviors of four ACFs: (a) during curing process, (b) during cooling process.

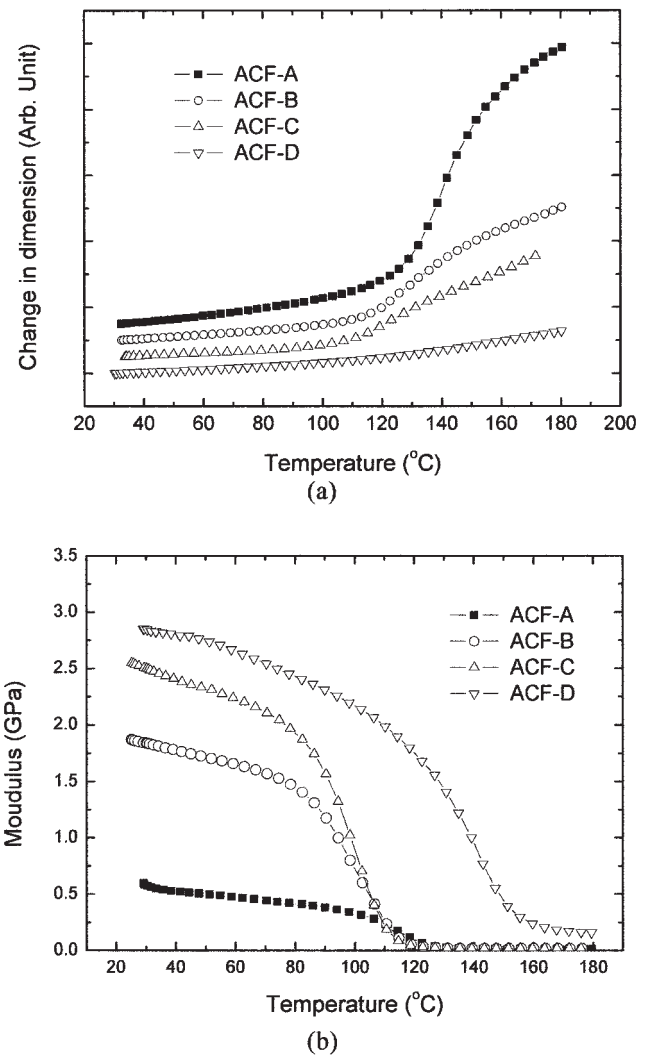


**Figure 6** Modulus changes of cured ACFs during cooling to room temperature.

### Thermal expansion and dynamic mechanical analysis of cured ACFs

Figure 6(a) shows the TMA curves of the four ACF materials under investigation. The inflection points of TMA curves may be defined as glass-transition points ($T_g$). Around these inflection points, there were shifts to higher CTE values because of changes in molecular free volume. The CTE values were calculated at the linear section of thermal expansion versus temperature, which ranged from 60 to 90°C. CTE values below inflection points are summarized in Table II.

**TABLE I**
**Comparison of Shrinkages During the Curing and Cooling Processes of ACFs**

| Material | Curing shrinkage[a] (%) | Cooling shrinkage[b] (%) |
|---|---|---|
| ACF-A | 2.32 | 7.35 |
| ACF-B | 1.67 | 5.21 |
| ACF-C | 1.46 | 4.37 |
| ACF-D | 1.79 | 3.86 |

[a] Occurred during the curing process.
[b] Estimated from 180°C to room temperature.

Figure 6(b) shows the temperature dependency of storage modulus for all the ACFs studied. The storage modulus of ACF materials increased as the temperature decreased. In particular, the storage modulus increased significantly near the glass-transition region, which is the well-known effect of the storage modulus increase of nearly two orders of magnitude below the temperature region associated with glass-transition temperature. That is, the elastic modulus exhibited a significant increase as the epoxy matrix underwent solidification below the glass-transition region. During the subsequent cooling period, the storage modulus reached different plateau values with ACF mate-

**TABLE II**
**Material Properties of Studied ACFs**

| Material | $T_g$ (°C) | CTE[a] (ppm/K) | Storage modulus[b] (GPa) | Poisson's ratio[c] |
|---|---|---|---|---|
| ACF-A | 118.7 | 97.1 ± 8.9 | Temperature dependent | 0.4 |
| ACF-B | 106.6 | 65.2 ± 5.3 | Temperature dependent | 0.4 |
| ACF-C | 107.9 | 50.8 ± 3.8 | Temperature dependent | 0.4 |
| ACF-D | 148.7 | 57.8 ± 3.4 | Temperature dependent | 0.4 |

[a] Measured (TMA).
[b] Measured (DMA).
[c] Estimated.

rials. The $T_g$ is the point at which ACF materials change from a hard, glassy material to a soft, rubbery one. Actually, glass transition occurs within a range of temperatures and not at a single point. Different methods of measurement for the glass-transition temperature also provide varying data for the same material. Therefore, the $T_g$ value can be defined in different ways with different values. The glass-transition temperature may correspond to the inflection point in the TMA curve. Moreover, it can be determined as either the peak temperature of loss tangent or the transition midpoint of the storage modulus curve in DMA analysis. From the mechanical viewpoint of stress build-up, glass-transition temperatures were defined as the inflection points between rubbery region and glass-transition region in Figure 6(b).

### Internal stress build-up behavior with the thermomechanical properties of ACFs

As described previously, ACF interconnections are mechanically constructed by the contraction stress that develops along the $z$-axis of ACF. The development of contraction stress is generally governed by the evolution of thickness contraction and mechanical stiffness during the curing and cooling processes.

Based on the incremental approach to linear elasticity, the contraction stress ($\sigma$) along the $z$-axis can be expressed as an integral of the thickness contraction and elastic modulus as

$$\sigma_z = \int_T E \, d\varepsilon_z \tag{1}$$

where $E$ is the temperature-dependent modulus and $\epsilon_z$ denotes the thickness contraction of ACFs.

In analyzing eq. (1), it should be noted that cure shrinkage after the completion of curing reaction was less than the cooling shrinkage, and the rubbery modulus was virtually zero compared with glassy modulus. Accordingly, the magnitude of contraction stress that occurred in the curing reaction is practically insignificant.[8] Therefore, this study focused on the build-up behavior of contraction stress in the cooling process.

Modulus change and thickness contraction during the cooling history can be simultaneously plotted with changing temperature. Modulus versus thickness contraction curves during the cooling process for four ACF materials are presented in Figure 7. Each starting point in these curves individually corresponds to the maximum temperature (180°C). Based on the incremental approach to linear elasticity, the evolution of contraction stresses with decreasing temperature is proportional to the area of modulus versus thickness contraction curve for the cooling process.

Figure 8 shows contraction stresses that developed during the cooling process, estimated by numerical integration according to eq. (1), as a function of temperature.

Upon cooling ACF from the bonding temperature to $T_g$, the contraction stress was almost negligible because ACFs in the rubbery state had an extremely low modulus. At lower than the $T_g$ of ACFs, contraction stress gradually started to grow as a result of the cooling shrinkage and significant increase in glassy modulus. It is evident that contraction stress during

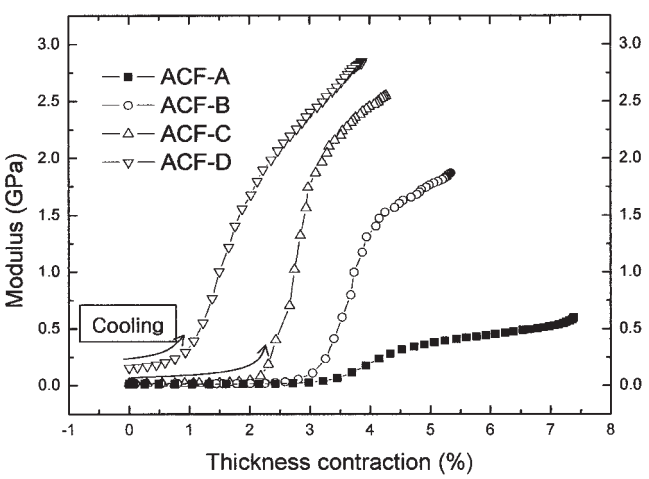


**Figure 7** Modulus ($E$) versus thickness contraction ($d\epsilon_z$) during cooling process. The area under the curve corresponds to the shrinkage stress.

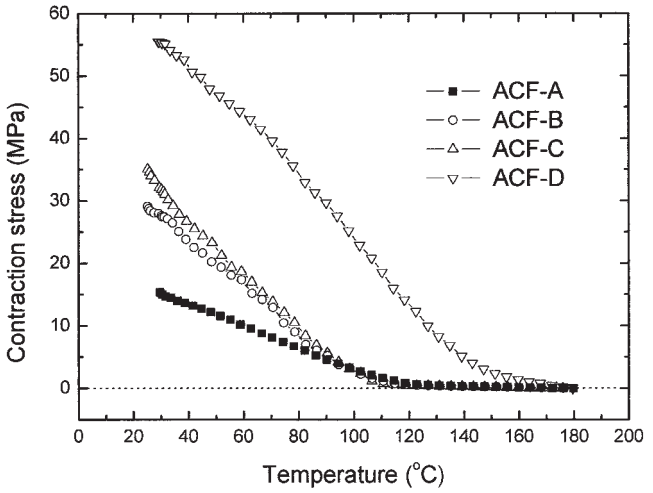


**Figure 8** Estimated contraction stresses along *z*-axis during the cooling process. Stress is calculated by numerical integration, according to eq. (1).

the ACF bonding process is primarily attributed to the cooling process below $T_g$. Therefore, the glass-transition temperature is the important determinant for estimating the contraction stress level in an ACF joint. After the evolution of the contraction stresses had begun at $T_g$, the stresses started to build up linearly with decreasing temperature below $T_g$. For the ACF materials studied, the difference in growth behaviors of contraction stresses below $T_g$ is clearly visible in Figure 8. That is, the increasing rates of contraction stresses characterized by linear slope below $T_g$ may be strongly dependent on materials properties: coefficient of thermal expansion (CTE), elastic modulus ($E$), and glass-transition temperature ($T_g$). The elastic modulus and thermal expansion coefficients are summarized in Table I. To examine the relationship between growth behavior of contraction stresses and materials characteristics, the increasing rates of contraction stresses below $T_g$ were correlated with the products of modulus and thermal expansion coefficient for each ACF material. Figure 9 clearly shows that a linear relationship exists between the experimental increasing rate and $E \times$ CTE, regardless of glass-transition temperature. The small deviation of the data from the fitted line may be caused by the slight discrepancy between the actual Poisson's ratio and the assumed Poisson's ratio. This result indicates that the growth behavior of contraction stress is closely correlated with the ACF material properties: CTE, glassy modulus, Poisson's ratio, and $T_g$.

### Electrical behavior of ACF contact during the cooling process

To investigate the electrical characteristics of ACF contact with cooling the assembly, *in situ* contact resistance was measured with temperature. The ACF used for the ACF flip-chip assembly was ACF-B. Figure 10 shows the changes of contact resistance of ACF contact with decreasing temperature.

During the cooling process, from 160 to 100°C, contact resistance of the ACF joint gradually increased, as shown in Figure 10, which originated from the cracking of the metal coating layer of gold-coated polymer spheres during the cooling process. However, during cooling below 100°C, contact resistance gradually decreased. With increasing cooling cycles, the contact resistance of ACF contact increased as a result of damage to the coating layer. It should be noted that electrical conduction of the ACF joint is robustly maintained by large contraction stress during the cooling process below 100°C.

## CONCLUSION

The cure shrinkage attributed to the crosslinking of epoxy chains transitionally increased with the progress of curing and attained constant degrees of shrinkage, ranging from 1.5 to 2.0%, when the curing reaction was completed. During the cooling process, four ACFs under investigation exhibited substantial cooling shrinkage, represented by a straight line having one inflection point, compared with cure shrinkage. Based on the incremental approach to linear elasticity, the full temperature evolution of contraction stresses of ACFs was experimentally shown by the thermal shrinkage and thermomechanical properties of ACF. The significant development of contraction stress occurred as a consequence of the cooling process below $T_g$. The ACF contact resistance during the cooling process revealed that electrical conduction of the ACF joint is robustly maintained by the large

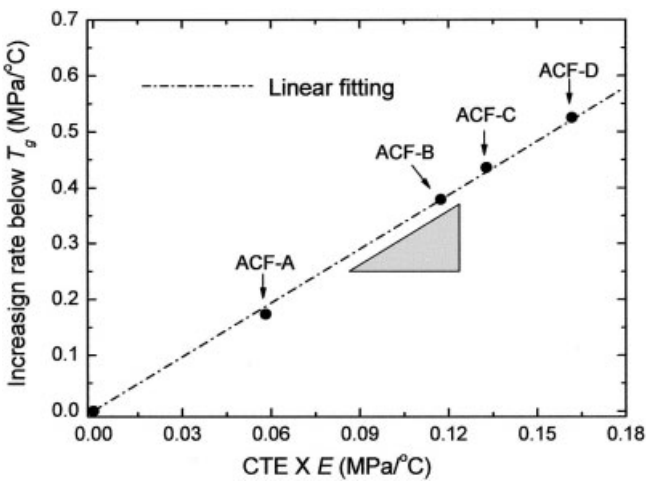


**Figure 9** Relation between observed increasing rates of contraction stress and calculated CTE $\times$ modulus in the cooling process below $T_g$.

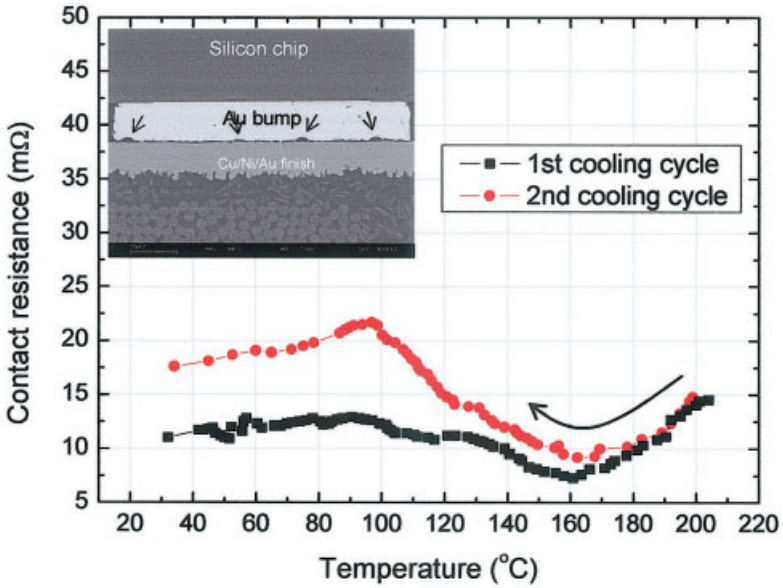


**Figure 10** Measured contact resistance of ACF contact structure during the cooling process.

contraction stress below $T_g$. The growth rate of contraction stress with decreasing temperature below $T_g$ was closely correlated with the ACF material properties: thermal expansion coefficient and glassy modulus. Therefore, it is considered that glass-transition temperature, CTE, and modulus are the important determinants for the development of contraction stress resulting in a reliable ACF joint. Based on the incremental approach to linear elasticity, we have shown the full temperature evolution of contraction stresses of ACFs, provided that the thickness shrinkage and modulus are determined as a function of temperature. Therefore, it is possible to estimate the amount of contraction stress build-up during the cooling process in a wide range of ACFs from the material characteristics of thermal shrinkage, elastic properties, and $T_g$.

## References

1. Liu, J. Mater Technol 1995, 10, 247.
2. Yim, M. J.; Paik, K. W.; Kim, Y. K.; Hwang, H. N. Advances in Electronic Packaging; EEP: New York, 1997; Vol. 19-1, 65.
3. Fu, Y.; Wang, Y.; Wang, X.; Liu, J.; Lai, Z. IEEE Trans Compon Pack T Part B: Adv Pack 2000, 23, 15.
4. Lai, Z.; Liu, J. IEEE Trans Compon Pack T Part B: Adv Pack 1996, 19, 644.
5. Plepys, A. R.; Farris, R. J. Polymer 1990, 31, 1932.
6. Ochi, M.; Yamashita, K.; Yoshizumi, M.; Shimbo, M. J Appl Polym Sci 1989, 38, 789.
7. Ochi, M.; Yamashita, K.; Shimbo, M. J Appl Polym Sci 1991, 43, 2013.
8. Kwon, W. S.; Paik, K. W. Int J Adhes Adhesives 2004, 24, 135.